15418

DRAFT

Heavily-shocked and brecciated Granulite

1141 grams

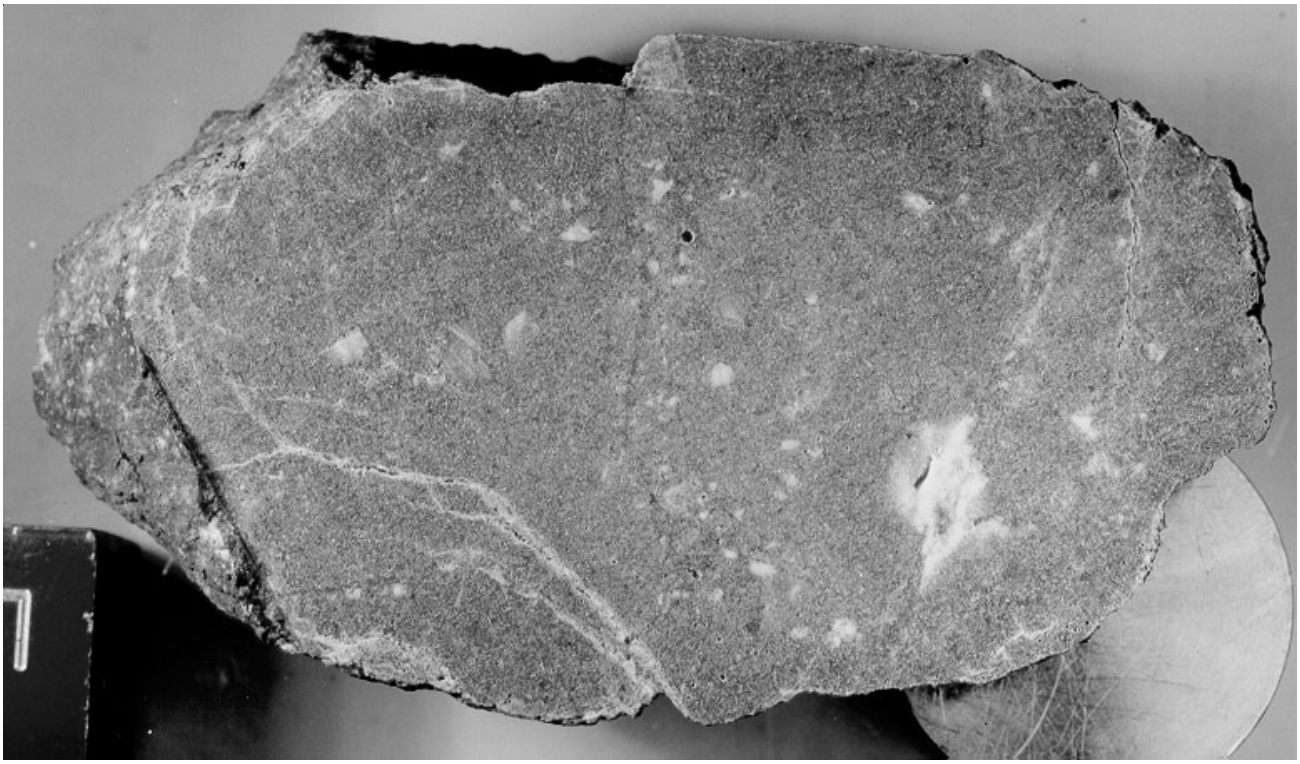

Figure 1: Sawn surface of 15418,27. Note sealed fractures. Sample is 12 cm long. Cube is 1 in. NASA S75-33763.

Introduction

Lunar sample 15418 is a highly-shocked, granulitic breccia that has a chemical composition of "gabbroic anorthosite" – and has, from time to time, been considered as representative of a portion of the original lunar crust. Although this sample has had a complicated history, the original metamorphic mineralogy with two pyroxenes can be identified. 15418 is highly aluminous (Al_2O_3 = 26%) and the potassium content is low (K = 0.01%). Lindstrom and Lindstrom (1986) have reviewed lunar granulites, in general, and 15418, in particular.

15418 has been dated at 4.04 b.y., with an exposure age of 250 m.y. It has micrometeorite craters on all sides.

Petrography

Four lithologies have been identified in 15418 (Nord et al. 1977, Cohen et al. 2004). The interior and main mass (figures 1 and 6) is a highly shocked, and previously brecciated, lunar granulite composed of ~70% anorthite and ~30% mafic (augite, orthopyroxene and olivine). In places within the rock the shock-melted, plagioclase has partially reacted with the mafic minerals (figure 2). Part of the sample is coated with aluminous glass which has recrystallized in places (figure 5). An area of highly vesicular glass is found on one side (figure 10). A penetrating fracture separated a high vesicular part of the rock from a more dense portion (figure 4). Vesicles in this outer zone, were up to a cm in size. This smaller piece (,1 to ,6) is what was initially studied in PET and from which most of the thin sections and initial reports were made.

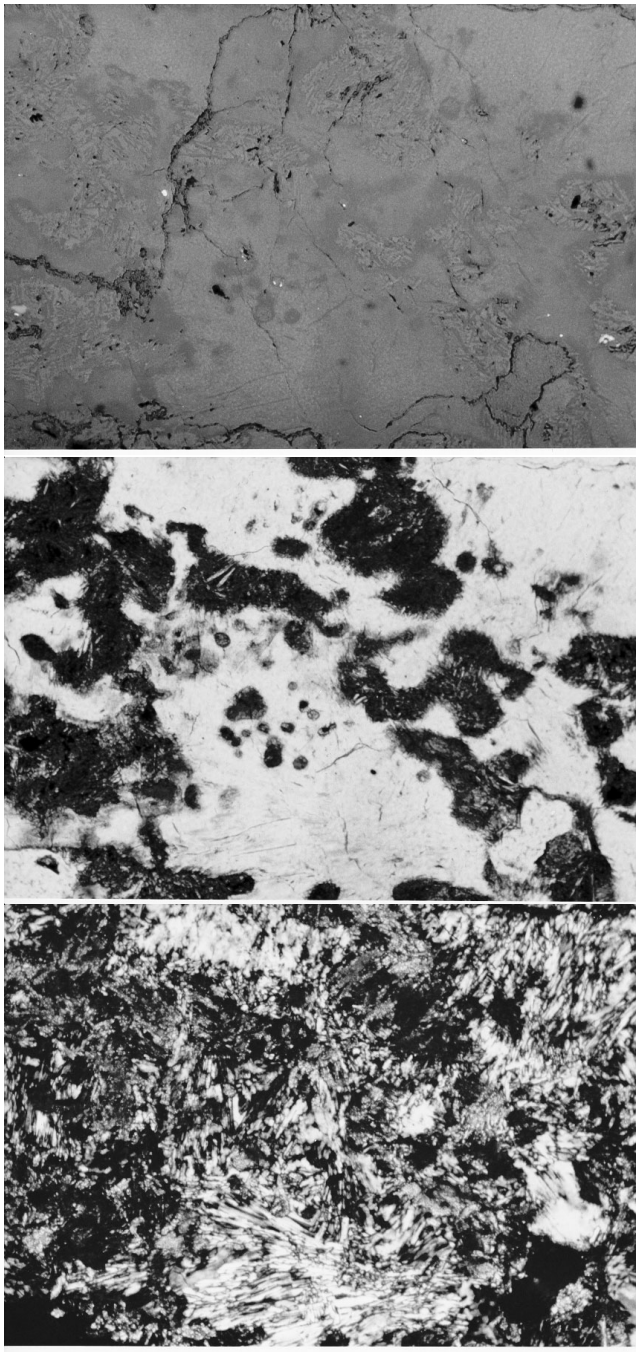

Figure 2: Photomicrographs of thin section ,24 from 15418. Scale is 1.3 mm across. NASA #S79-27452-454. Top is reflected light, middle is transmitted light, bottom is with crossed-polarizer.

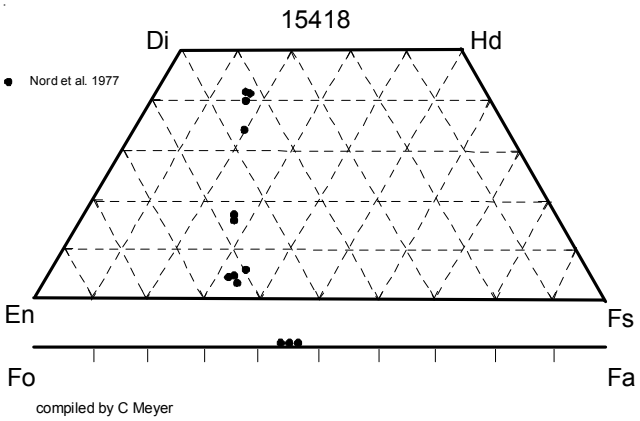

Figure 3: Pyroxene and olivine composition of 15418 (from Nord et al. 1977).

Sample 15418 was extensively studied to characterize microstructures in minerals and glass (Heuer et al. 1972, Christie et al. 1973, Gleadow et al. 1974, Nord et al. 1977). At high magnification it was found that many mineral grains in 15418 have a high density of tiny pores (an unusual feature). The substructures of the minerals in 15418 suggest severe shock deformation.

The interior portion of 15418 has a texture of a shocked granulitic breccia that originally had a relatively coarse granoblastic texture (Cohen et al. 2004). In places (zones), this original texture is obscured by subsequent shock-heating events. The outermost zone (rind) has a subophitic-intergranular texture and may represent a portion of a thicker rind that is no longer present (Cohen et al. 2004).

The part of the exterior of 15418 that was originally described by LSPET (1972) is different from the interior of the sample. It includes an outer zone of flow-banded glass, with various areas of devitrifcation and recrystallization (figure 5).

According to Cohen et al. (2004), "15418 was originally a relatively-coarse grained granoblastic granulitic breccia". The main mass of 15418 was shocked to an extent that all the plagioclase was converted to maskelynite (30-40 GPa). Later it was coated by a high-temperature, high-shock-pressure, aluminous melt that caused the interior maskelynite to partially recrystallize and caused small vesicles in the resulting plagioclase.

Mineralogy

Olivine: The chemical composition of olivine is Fo_{52-57} (Nord et al. 1977). Olivine grains are found to have a high density of dislocations (Heuer et al. 1972).

Figure 4: Original photo of 15418 showing a few zap pits and a penetrating fracture. Note the portion of a very large vesicle on the bottom. NASA S71-44865. Sample is 11 cm long.

Pyroxene: The compositions of primary augite and orthopyroxene are plotted in figure 3.

Plagioclase: Some plagioclase crystals in 15418 have aggregate extinction between crossed polarizers, resembling single crystals, but at higher magnification have a fine-grained polycrystalline structure (Heuer et al. 1972). Much of the plagioclase has been shocked to maskelynite and/or to glass. The composition of plagioclase is uniform at $An_{96\text{-}97}$.

Glass: Anorthite glass has recrystallized, often in spherulitic or rounded fibrous structures (Heuer et al. 1972). According to Cohen et al. (2004) the bulk composition of the glass is not the same as for the whole rock.

High-pressure phases: Although, Cohen et al. (2004) find that the outer portion of 15418 may have been shocked to greater than 100 GPa, no relict, high-pressure phases have been reported.

Chemistry

Laul et al. (1972), Bansal et al. (1972), Taylor et al. (1973), Lindstrom and Lindstrom (1986), Weismann and Hubbard (1977) and others reported chemical analyses (table 1, figure 8).
The sample is highly aluminous with low trace element content. Ganapathy et al. (1973) found that the pieces they analyzed were high in meteoritic siderophiles (Ir and Au). It is important that chemical composition be correlated with the portion of the rock studied.

Schonfeld (1975) used the composition of 15418 to model the composition of the lunar crust.

Radiogenic age dating

Stettler et al. (1973) dated 15418,50 by the Ar/Ar plateau technique at 4.04 ± 0.06 b.y. (figure 9).

Cosmogenic isotopes and exposure ages

Stettler et al. (1973) determined an exposure age of 250 m.y. by ^{37}Ar. Keith et al. (1972) determined cosmic ray induced activities of ^{26}Al = 120 dpm/kg., ^{22}Na = 27 dpm/kg., ^{54}Mn = 8 dpm/kg, ^{56}Co = 1.9 dpm/kg. and ^{46}Sc = 0.8 dpm/kg.

Figure 5: Recrystallized glass from 15418. NASA S71-51743.

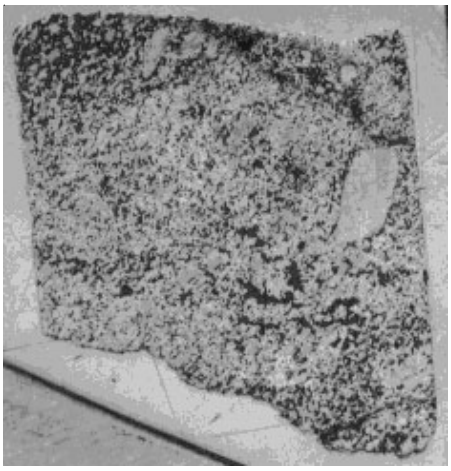

Figure 6: Thin section 15418,152. Scale 1 cm.

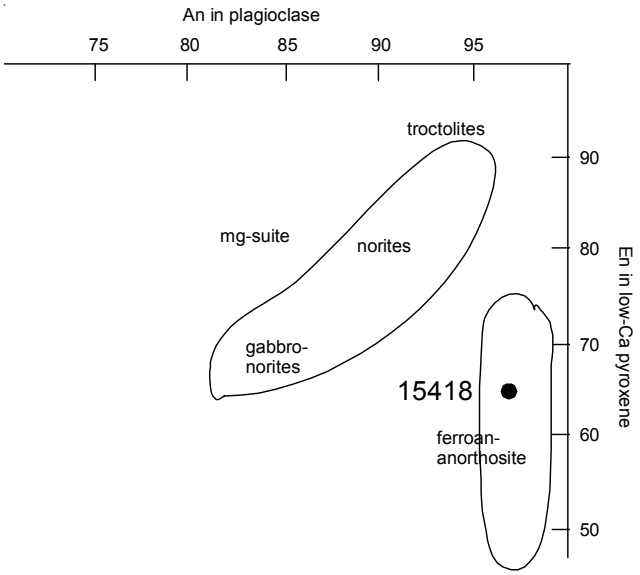

Figure 7: Composition of plagioclase and mafic minerals in 15418.

Other Studies

Ahrens et al. 1973	shock measurements
Allen et al. 1973	204Pb
Baldridge et al. 1972	thermal expansion
Cukiermann and Uhlmann 1972	glass flow
Hutcheon et al. 1972	gas bubbles
Huffman et al. 1972	Mossbauer
Keith and Clarke 1972	cosmogenic isotopes
MacDougall et al. 1973	no solar flare tracks
Nagata et al. 1972, 1973, 1975	magnetic properties
Nyquist et al. 1972, 1973	Sr isotopes
O'Keefe and Ahrens 1975	equation of state
Richter et al. 1976	microcracks
Schwerer et al. 1973	Mossbauer
Schwerer et al. 1974	electrical conductivity
Tatsumoto et al. 1972	Pb isotopes
Todd et al. 1973	seismic velocity
Uhlmann et al. 1974	glass flow
Wang et al. 1973	seismic velocity
Yinnon et al. 1980	glass flow, DTA

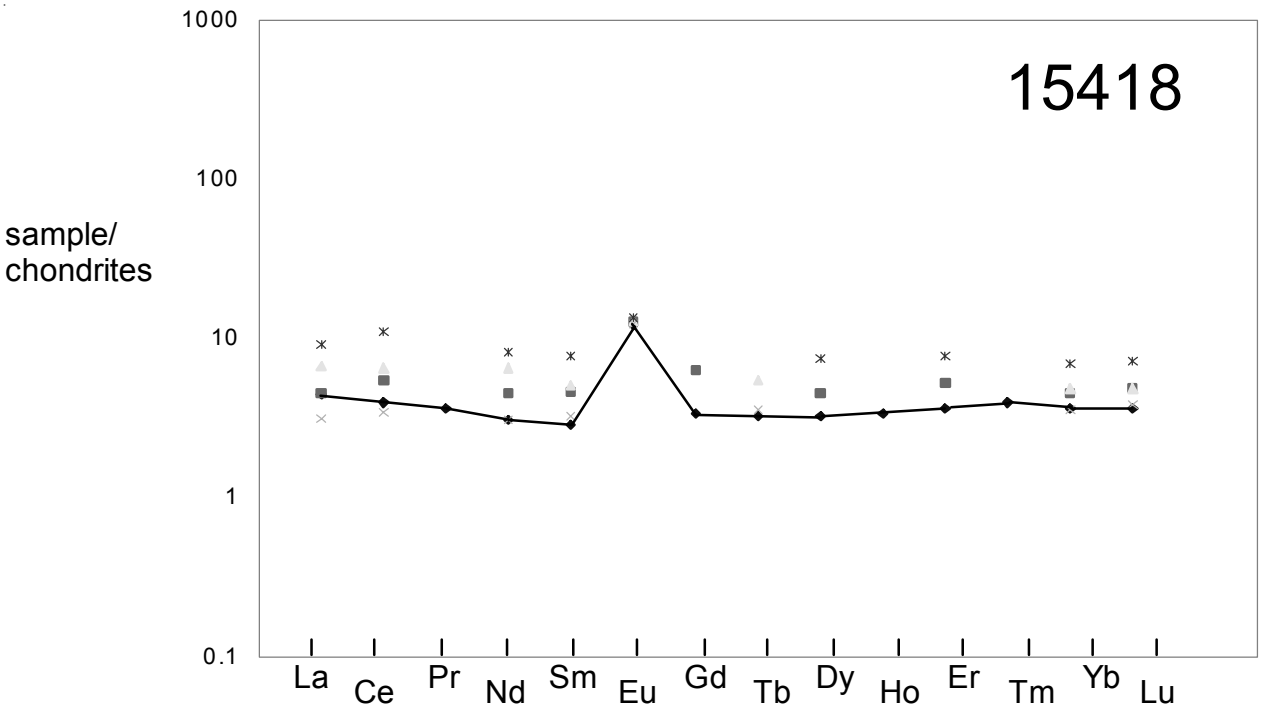

Figure 8: Normalized rare earth element diagram for 15418 (data from Taylor et al. 1973 connected. Addtional data from Wiesmann et at., Bansal et al., Laul et al. and Lindstrom and Lindstrom - see table).

Processing

A bandsaw was used in a dry nitrogen cabinet to cut a slab (,28) which was further subdivided into a column (,31) and end pieces (figure 11). The width of the slab was ~1.5 cm and the width of the column (,31) was ~2 cm. The column was split lengthwise (,32 and ,33) and cut into cubes with many fine cuts (figures 13 and 41). Thin sections were made from different parts of 15418, show different lithologies (see diagram). Figures 1 and 6 illustrate the main shocked granultitic lithology.

Ryder (1985) gives a full description of the research performed on 15418 up to that time. It is apparent that 15418 needs to be studied in "consortium mode" – as was done for complicated samples in later missions. Cohen et al. (2004) compared 15418 with one of the lunar meteorites (Dhofar 026). This comparison strengthens the case that 15418 may be representative of the lunar crust. But, clearly, the main interior lithology of 15418 deserves a more coordinated and methodical study.

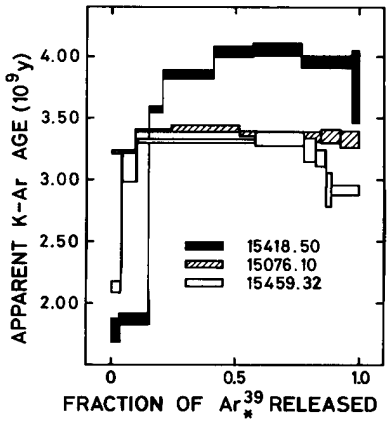

Figure 9: Ar/Ar plateau age for 15418,50 (from Stettler et al. 1973).

Summary of Age Data for 15418

	Ar/Ar
Stettler et al. 1973	4.04 ± 0.06 b.y. (intermediate temperature plateau)
Stettler et al. 1973	3.99 ± 0.07

Table 1. Chemical composition of 15418.

			sawdust	sawdust							sawdust			
reference	*LSPET 72*		Laul 72	Laul 83	Lindstrom 86						Wiesmann 77			
weight			147 mg								56 mg	50 mg	54 mg	
SiO2 %	44.97	(c)												
TiO2	0.27	(c)	0.37	0.3	0.41	0.25			0.25	(a)	0.27	0.23	0.27	(b)
Al2O3	26.73	(c)	26.4	26.4	25.7	26.8			28.4	(a)				
FeO	5.37	(c)	7.5	7	4.9	6.44	6.84	6.52	5.11	(a)				
MnO	0.08	(c)	0.086		0.077	0.09			0.077	(a)				
MgO	5.38	(c)	5.3	6	6.4	5.5			4.3	(a)				
CaO	16.1	(c)	15.8	15.7	15.4	15.6	15.4	15.7	16.5	(a)	15.8			(b)
Na2O	0.31		0.282	0.29	0.39	0.29	0.27	0.27	0.3	(a)	0.27	0.32	0.3	(b)
K2O	0.03		0.011							(a)	0.013	0.02	0.024	(b)
P2O5	0.03	(c)												
S %	0.03	(c)												
sum														
Sc ppm			12.7	12	9.11	11.8	13.4	13.5	10.5	(a)				
V			42											
Cr	752	(c)	1916	1920	818	690	870	882	639	(a)		614	628	(b)
Co			77	70	15.7	11	13.5	14.7	7.8	(a)				
Ni				700	125	36	65	45	26	(a)				
Cu														
Zn														
Ga														
Ge ppb														
As														
Se														
Rb											0.17	0.361	0.489	(b)
Sr	152	(c)			161	138	150	135	149	(a)	140	148	139	(b)
Y														
Zr	67	(c)			110	25	<50	<50	<45	(a)	18	30	35	(b)
Nb														
Mo														
Ru														
Rh														
Pd ppb														
Ag ppb														
Cd ppb														
In ppb														
Sn ppb														
Sb ppb														
Te ppb														
Cs ppm					0.11	<0.05	<0.05		<0.05	(a)				
Ba			70	30	100	19	15	14	15	(a)	19.2	24.4	28.9	(b)
La			1.2	1.6	8.02	0.759	0.756	0.812	0.719	(a)	1.07	1.73	2.19	(b)
Ce				4	20.8	2.1	2.05	2.22	1.86	(a)	3.31		6.78	(b)
Pr														
Nd				3	12.5	1.4	1.6	1.2	1.3	(a)	2.09	3.15	3.75	(b)
Sm			0.69	0.75	3.74	0.485	0.499	0.541	0.437	(a)	0.688	0.94	1.16	(b)
Eu			0.73	0.726	0.911	0.697	0.698	0.699	0.696	(a)	0.726	0.764	0.762	(b)
Gd											1.25	1.25		(b)
Tb			0.18	0.2	0.88	0.129	0.149	0.15	0.129	(a)				
Dy			1.2							(a)	1.12	1.49	1.84	(b)
Ho														
Er											0.85	1.04	1.24	(b)
Tm														
Yb			0.81	0.8	2.9	0.593	0.628	0.65	0.55	(a)	0.74	0.907	1.12	(b)
Lu			0.12	0.12	0.444	0.094	0.102	0.105	0.085	(a)	0.12	0.143	0.176	(b)
Hf			0.8	0.7	2.78	0.36	0.4	0.42	0.32	(a)	0.5	0.8	0.6	(b)
Ta			0.09		0.32	0.033	0.031	0.04	0.026	(a)				
W ppb														
Re ppb														
Os ppb														
Ir ppb				<5	3.8	2.2	1.8	1	1	(a)				(b)
Pt ppb														
Au ppb				3	1.6	<1	<1	<1	<1	(a)				(b)
Th ppm				0.25	1.27	0.046	0.049	0.064	0.024	(a)				(b)
U ppm					0.33	<0.09	<0.1	<0.1	<0.06	(a)	0.045			(b)
technique	*(a) INAA, (b) IDMS, (c) XRF*													

Table 1b. Chemical composition of 15418.

reference	Bansal 72		Taylor 73		Hubbard 74		Ganapathy 73			Tatsumoto 72			Nyquist 73			Keith 72	
weight										sawdust							
SiO2 %	44.2	(c)			45.53	(c)											
TiO2	0.27	(c)			0.29	(c)											
Al2O3	26.6	(c)			25.98	(c)											
FeO	6.65	(c)			6.66	(c)											
MnO					0.1	(c)											
MgO	5.08	(c)			6.09	(c)											
CaO	16	(c)			15.63	(c)											
Na2O	0.27	(c)			0.31	(c)											
K2O	0.013	(c)			0.03	(c)				0.015						0.0104	(f)
P2O5					0.03	(c)											
S %					0.03	(c)											
sum																	
Sc ppm			7	(d)													
V			18	(d)													
Cr			1150	(d)													
Co			10	(d)													
Ni			54	(d)													
Cu			2	(d)													
Zn							0.82	0.49	(e)								
Ga			2.2	(d)													
Ge ppb							65	17	(e)								
As																	
Se							56	25	(e)								
Rb	0.17	(b)					0.8	0.03	(e)	0.263			0.162	0.361	(b)		
Sr	140	(b)								134.6			140.1	147.8	(b)		
Y																	
Zr																	
Nb			0.43	(d)													
Mo																	
Ru																	
Rh																	
Pd ppb																	
Ag ppb							0.59	1.4	(e)								
Cd ppb							1.7	2.4	(e)								
In ppb							0.29	0.18	(e)								
Sn ppb																	
Sb ppb							0.5	0.16	(e)								
Te ppb							3.7	1.9	(e)								
Cs ppm							0.04	0.008	(e)								
Ba	19.2	(b)	20	(d)													
La	1.07	(b)	1.06	(d)													
Ce	3.31	(b)	2.4	(d)													
Pr			0.33	(d)													
Nd	2.09	(b)	1.41	(d)													
Sm	0.688	(b)	0.43	(d)													
Eu	0.726	(b)	0.69	(d)													
Gd	1.25	(b)	0.67	(d)													
Tb			0.12	(d)													
Dy	1.12	(b)	0.8	(d)													
Ho			0.19	(d)													
Er	0.85	(b)	0.59	(d)													
Tm			0.1	(d)													
Yb	0.74	(b)	0.6	(d)													
Lu	0.12	(b)	0.09	(d)													
Hf			0.16	(d)													
Ta																	
W ppb																	
Re ppb							0.38	0.13	(e)								
Os ppb																	
Ir ppb							5.4	2.2	(e)								
Pt ppb																	
Au ppb							1	0.26	(e)								
Th ppm			0.1	(d)						0.208	0.127	0.1377			(b)	0.102	(f)
U ppm	0.045	(b)					0.185	0.024	(e)	0.058	0.038	0.0394			(b)	0.043	(f)

technique (a) INAA, (b) IDMS, (c) XRF, (d) ssms, (e) RNAA, (f) radiation counting

Figure 10: Photo of 15418,1 illustrating vesicularity. Large piece is 2 cm across. NASA S72-32321.

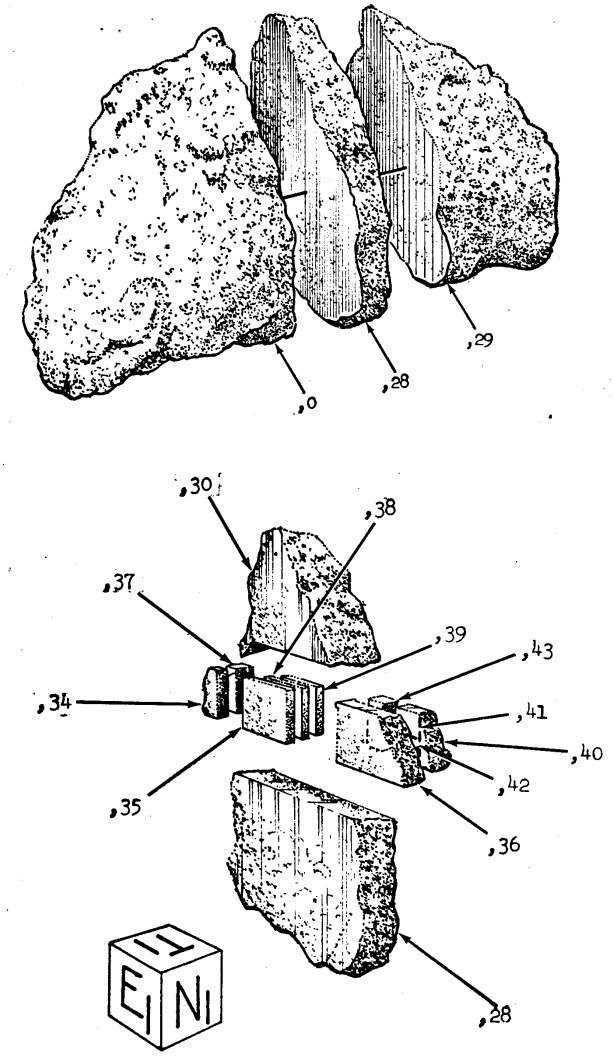

List of Photo #s for 15418

S71-51743	TS color
S71-52203	TS
S71-52498	TS
S71-43656 – 661	color mug
S71-44890 – 865	color mug
S71-45266 – 297	B&W mug
S71-59176 – 206	processing
S71-59591 – 610	processing
S71-59894 – 918	processing
S72-34093	,0 B&W
S72-32321	,1 vesicular
S75-33598	,27 vesicular
S75-33763	,27 sawn surface
S76-21675	,0 B&W
S79-27452 – 454	TS color
S81-29176 – 180	,167 color
S81-29203 – 209	,179 color

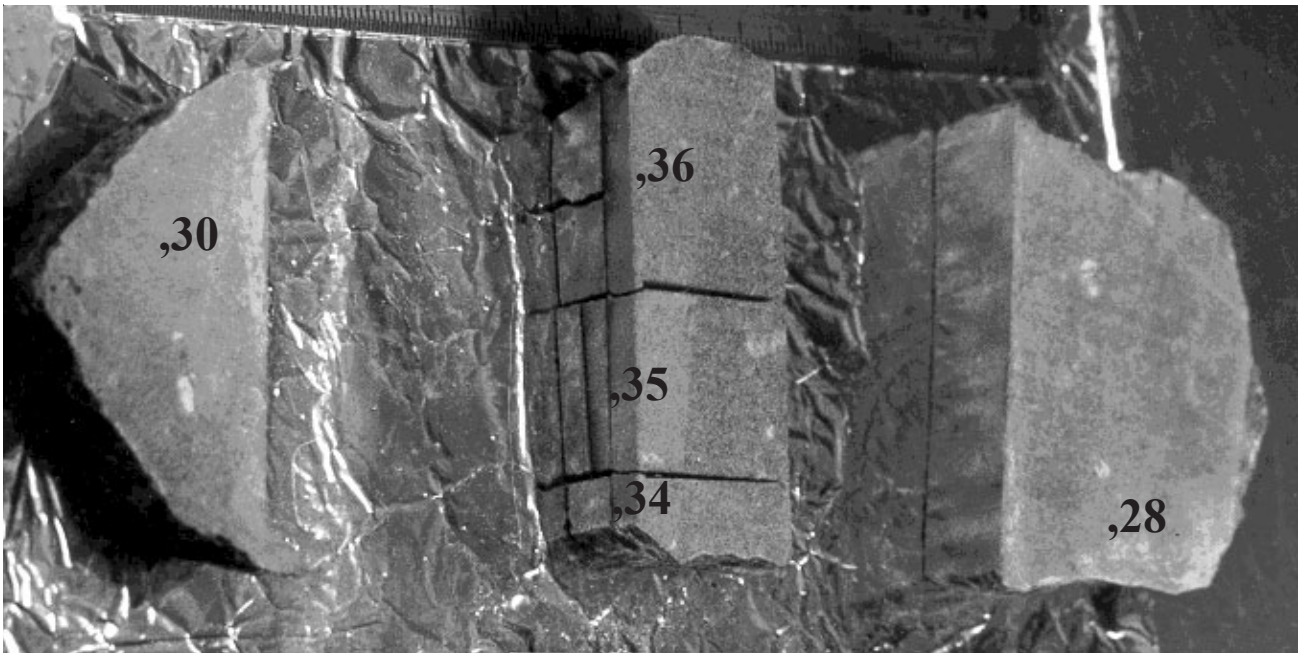

Figure 11: Subdivision of slab 15418,28. NASA S71-59606. Column is 2 cm wide.

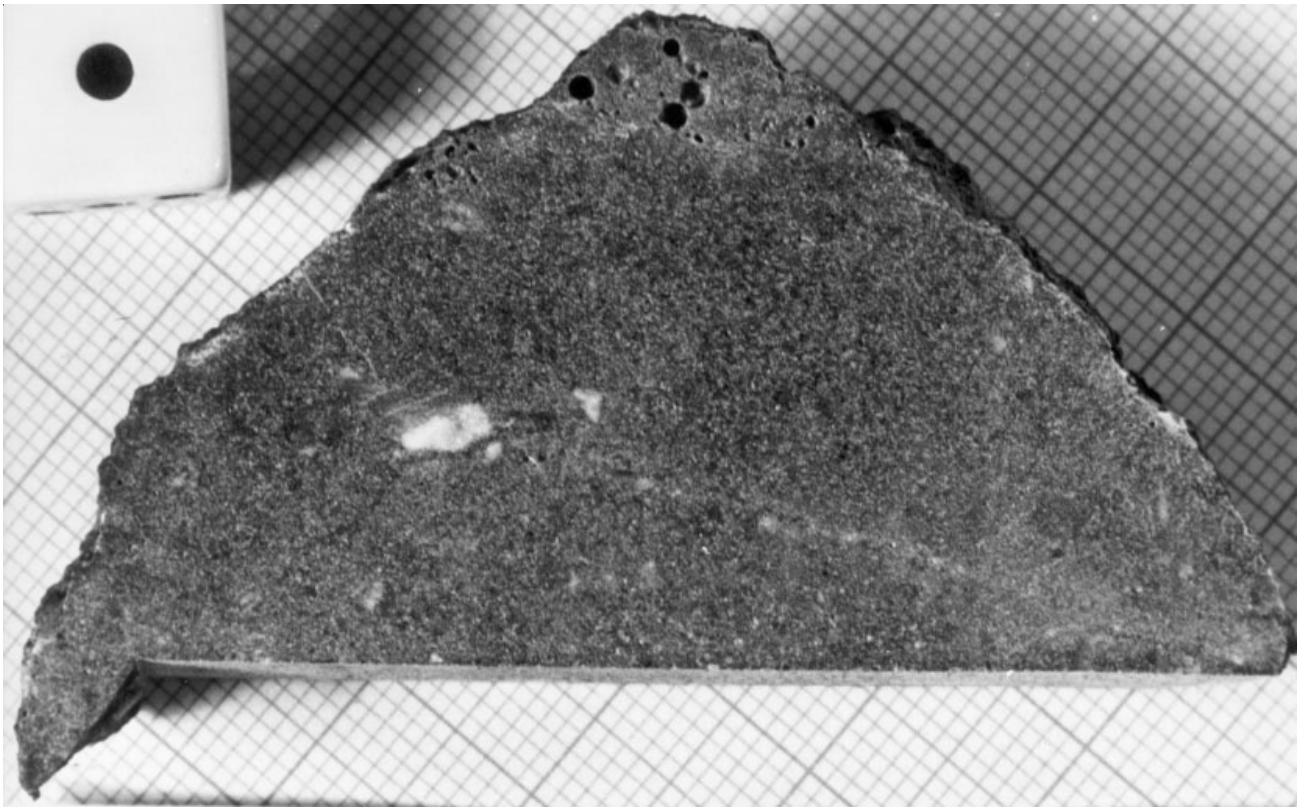

Figure 12: Mini-slab of 15418,30. Cm graph paper for scale. Photo by Tatsumoto.

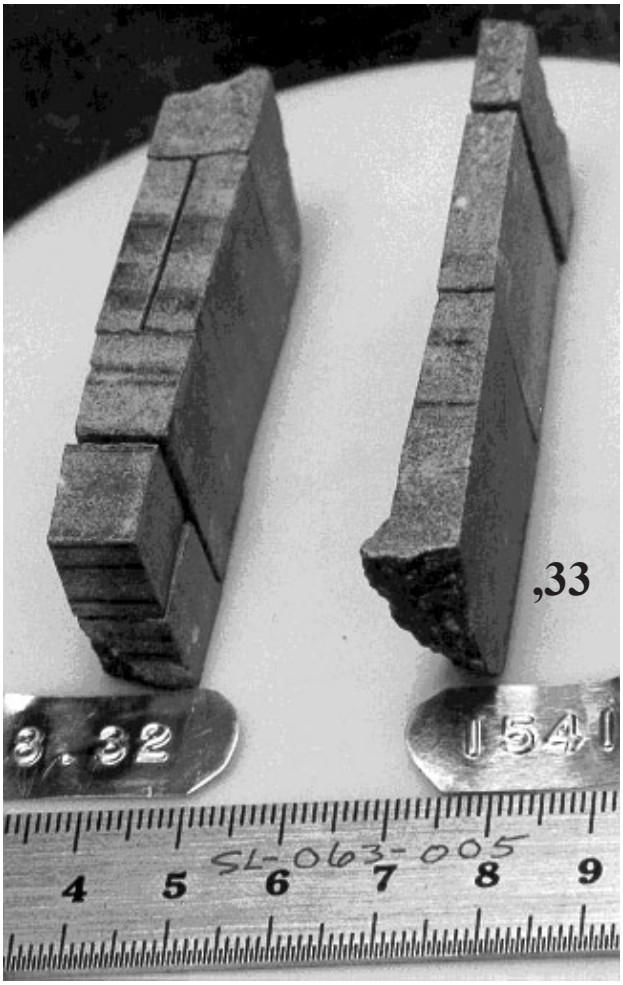

Figure 13: Splitting column 15418,31. S71-59604. Scale in cm.

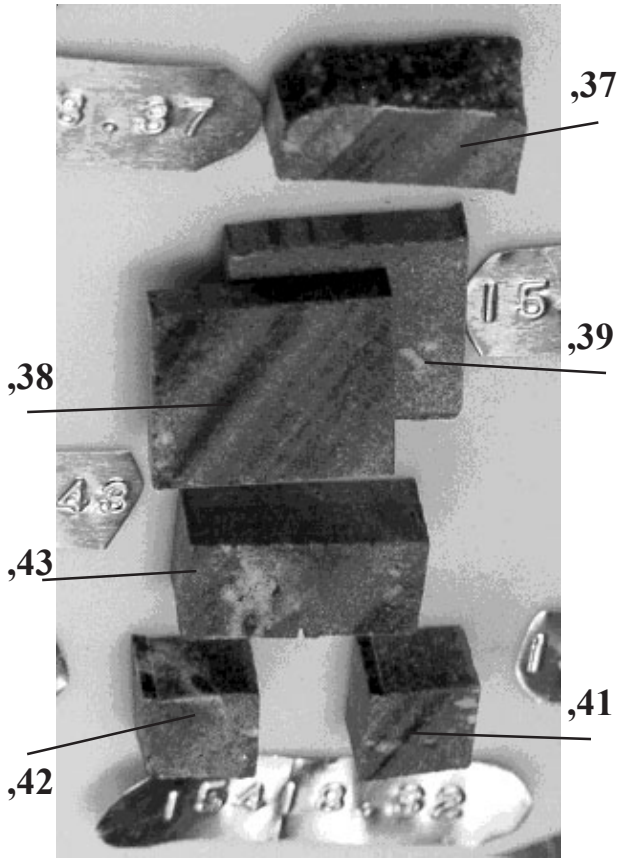

Figure 14: Cutting 15418,32 into cm cubes. S71-59918.